



A LETTERS JOURNAL EXPLORING
THE FRONTIERS OF PHYSICS

OFFPRINT

Pattern orientation in finite domains without boundaries

LISA RAPP, FABIAN BERGMANN and WALTER ZIMMERMANN

EPL, **113** (2016) 28006

Please visit the website
www.epljournal.org

Note that the author(s) has the following rights:

- immediately after publication, to use all or part of the article without revision or modification, **including the EPLA-formatted version**, for personal compilations and use only;
- no sooner than 12 months from the date of first publication, to include the accepted manuscript (all or part), **but not the EPLA-formatted version**, on institute repositories or third-party websites provided a link to the online EPL abstract or EPL homepage is included.

For complete copyright details see: <https://authors.eplletters.net/documents/copyright.pdf>.



A LETTERS JOURNAL EXPLORING
THE FRONTIERS OF PHYSICS

AN INVITATION TO SUBMIT YOUR WORK

www.epljournal.org

The Editorial Board invites you to submit your letters to EPL

EPL is a leading international journal publishing original, innovative Letters in all areas of physics, ranging from condensed matter topics and interdisciplinary research to astrophysics, geophysics, plasma and fusion sciences, including those with application potential.

The high profile of the journal combined with the excellent scientific quality of the articles ensures that EPL is an essential resource for its worldwide audience. EPL offers authors global visibility and a great opportunity to share their work with others across the whole of the physics community.

Run by active scientists, for scientists

EPL is reviewed by scientists for scientists, to serve and support the international scientific community. The Editorial Board is a team of active research scientists with an expert understanding of the needs of both authors and researchers.



OVER
560,000
full text downloads in 2013

24 DAYS
average accept to online
publication in 2013

10,755
citations in 2013

*"We greatly appreciate
the efficient, professional
and rapid processing of
our paper by your team."*

Cong Lin
Shanghai University

Six good reasons to publish with EPL

We want to work with you to gain recognition for your research through worldwide visibility and high citations. As an EPL author, you will benefit from:

- 1 Quality** – The 50+ Co-editors, who are experts in their field, oversee the entire peer-review process, from selection of the referees to making all final acceptance decisions.
- 2 Convenience** – Easy to access compilations of recent articles in specific narrow fields available on the website.
- 3 Speed of processing** – We aim to provide you with a quick and efficient service; the median time from submission to online publication is under 100 days.
- 4 High visibility** – Strong promotion and visibility through material available at over 300 events annually, distributed via e-mail, and targeted mailshot newsletters.
- 5 International reach** – Over 2600 institutions have access to EPL, enabling your work to be read by your peers in 90 countries.
- 6 Open access** – Articles are offered open access for a one-off author payment; green open access on all others with a 12-month embargo.

Details on preparing, submitting and tracking the progress of your manuscript from submission to acceptance are available on the EPL submission website www.epletters.net.

If you would like further information about our author service or EPL in general, please visit www.epljournal.org or e-mail us at info@epljournal.org.

EPL is published in partnership with:



European Physical Society



Società Italiana
di Fisica

Società Italiana di Fisica

 **EDP sciences**  **IOP Publishing**

EDP Sciences

IOP Publishing

Pattern orientation in finite domains without boundaries

LISA RAPP, FABIAN BERGMANN and WALTER ZIMMERMANN

Theoretische Physik I, Universität Bayreuth - 95440 Bayreuth, Germany

received 24 October 2015; accepted in final form 4 February 2016
published online 18 February 2016

PACS 89.75.Kd – Patterns

PACS 87.18.-h – Biological complexity

PACS 47.20.-k – Fluid instabilities

Abstract – We investigate the orientation of nonlinear stripe patterns in finite domains. Motivated by recent experiments, we introduce a control parameter drop from supercritical inside a domain to subcritical outside without boundary conditions at the domain border. As a result, stripes align perpendicularly to shallow control parameter drops. For steeper drops, non-adiabatic effects lead to a surprising orientational transition to parallel stripes with respect to the borders. We demonstrate this effect in terms of the Brusselator model and generic amplitude equations.

editor's choice Copyright © EPLA, 2016

Introduction. – Pattern formation is central to the wealth of fascinating phenomena in nature. It occurs in a great variety of physical, chemical and living systems [1,2]. Examples include patterns in isotropic and anisotropic convection systems [3–7], chemical reactions [8,9] and biological systems [10–12], or environmental patterns [13].

In real systems, patterns emerge in finite areas or volumes. Consequently, spatially periodic patterns only contain a finite number of wavelengths. Along the system borders, the relevant fields have to obey boundary conditions that influence the pattern in different ways [3,14–25]. In isotropic systems, stationary patterns may be oriented perpendicularly to the boundaries [3,15]. In thermal convection, convection rolls align perpendicularly to side walls due to boundary conditions for the flow fields [17–19]. Boundary conditions at the side walls may also restrict the range of possible stable wave numbers of periodic patterns [20]. Traveling waves of finite wave number may be reflected at the boundaries leading to a number of interesting and complex phenomena [21–25].

However, finite systems can also be achieved when the fluxes and forces driving a pattern, the so-called control parameters, are sufficiently strong (supercritical) only in a subdomain of the system. In this case, no specific boundary conditions act on the fields at *control parameter drops* to subcritical values. Related to this are studies of ramps in quasi-one-dimensional systems [26], whereby smooth ramps may lead to wave number selection [26,27] and rapid parameter changes to pinning effects for spatially periodic patterns [28]. But the effects of restricting two dimensional patterns to a finite domain by control parameter

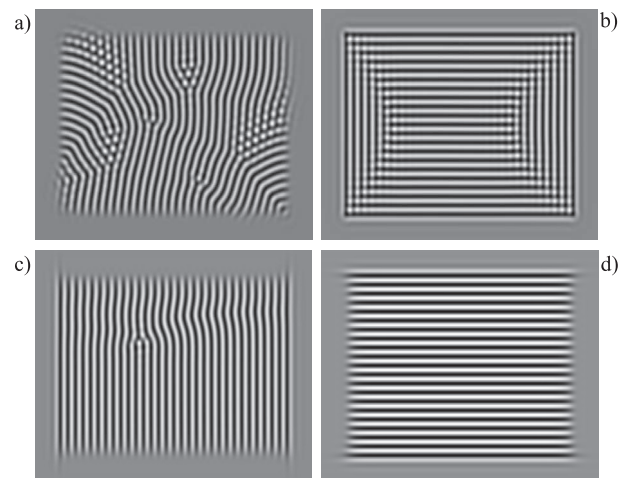


Fig. 1: Stripe patterns inside supercritical subdomains in the Brusselator model. The control parameter drops on different length scales $\delta_{x,y}$ along x and y from $\beta_m = 0.05$ to subcritical values in a wide vicinity: (a) $\delta_x = \delta_y = \lambda_c$, (b) $\delta_x = \delta_y = 0.32\lambda_c$, (c) $\delta_x = 0.32\lambda_c$, $\delta_y = 1.5\lambda_c$, (d) $\delta_x = 1.5\lambda_c$, $\delta_y = 0.32\lambda_c$.

drops have not been systematically investigated so far. Examples of pattern orientations resulting from different widths of the control parameter drops are shown in fig. 1 and explained in this work.

Recent experiments where pattern forming protein reactions take place in finite subdomains of substrates [29] belong to this class. Control parameter drops can also be designed in light-sensitive chemical reactions where illumination of the reaction cell suppresses pattern

formation [30,31]. If the illumination is only applied to a subdomain of the system, again no boundary conditions for the concentration fields are defined along the edge of the illumination mask.

We investigate how control parameter drops along the borders of a supercritical subdomain affect the orientation of stationary spatially periodic patterns when no boundary conditions for the fields are specified. We choose the Brusselator as a representative model system to study the influence of the control parameter drop width. This is complemented by studies of the so-called amplitude equations for supercritical bifurcations to spatially periodic patterns [3]. As a general description for this class of patterns, the conclusions drawn from the amplitude equations emphasize the universality of our results.

For large drop widths, we find that stripes align perpendicularly to the borders of the supercritical control parameter domain. By decreasing the length scale for the control parameter drop, we find a surprising orientational transition to stripes in parallel alignment. The analysis of the amplitude equations reveals additional non-adiabatic, resonance-like effects favouring parallel stripes.

Model systems and control parameter drop. –

Brusselator. The Brusselator is a common model for reaction-diffusion systems [32–35]. We use it as a prototype system for supercritical bifurcations to spatially periodic patterns (Turing patterns). It describes the nonlinear behaviour of the concentration fields $u(x, y, t)$ and $v(x, y, t)$:

$$\partial_t u = \nabla^2 u + a - (b + 1)u + u^2 v, \quad (1a)$$

$$\partial_t v = D \nabla^2 v + bu - u^2 v, \quad (1b)$$

with the *control parameter* b and constant parameters a , D . These equations have the homogeneous fixed point solution

$$u_h = a, \quad v_h = b/a. \quad (2)$$

Turing patterns with the critical wave number q_c bifurcate from this basic state for control parameter values beyond its critical one b_c [34], where

$$b_c = (1 + a\eta)^2, \quad q_c = \sqrt{a\eta}, \quad (3)$$

and $\eta := \sqrt{1/D}$. The relative distance β of the control parameter from its critical value b_c is given by

$$b = b_c(1 + \beta), \quad (4)$$

i.e. $\beta_c = 0$. Hexagons are typical for the Brusselator near the onset of Turing patterns. But in this work, we consider the special case $D = a^2$ where stripes are preferred at the onset [35]. In this case, the critical wavelength of the stripes according to eq. (3) is $\lambda_c := 2\pi/q_c = 2\pi$. We choose $a = 4$ throughout this work.

Amplitude equations. The two concentration fields u and v may be combined to the vector field $\mathbf{w}(\mathbf{r}, t) = (u(\mathbf{r}, t), v(\mathbf{r}, t))$. We write spatially periodic stripes with the wave vector \mathbf{q}_c in the form [3,34]

$$\mathbf{w}(\mathbf{r}, t) = \mathbf{w}_h + A \tilde{\mathbf{w}} e^{i(\mathbf{q}_c \cdot \mathbf{r})} + A^* \tilde{\mathbf{w}}^* e^{-i(\mathbf{q}_c \cdot \mathbf{r})}, \quad (5)$$

where $\mathbf{w}_h = (u_h, v_h)$. Slow variations (compared to the wavelength λ_c) of the envelope $A(\mathbf{r}, t)$ can be described by a dynamical amplitude equation [3,36].

The Brusselator model is isotropic. Hence, in extended systems only the magnitude q_c of the critical wave vector \mathbf{q}_c for Turing stripes is fixed, but not its direction. Thus, all stripe orientations are equally likely at pattern onset. We consider the amplitude equations in two limits of stripe orientations: $\mathbf{q}_c = (q_c, 0)$ and $\mathbf{q}_c = (0, q_c)$, called parallel and perpendicular hereafter. The reduction method to amplitude equations, the so-called multiple scale analysis, is well established for supercritical bifurcations [3,36]. The generic amplitude equations for the two stripe orientations in the case of a small and constant control parameter β are

$$\partial_t A = \beta A + \mathcal{L}A - g|A|^2 A, \quad (6)$$

with

$$\mathcal{L} = \mathcal{L}_{\parallel}^2 := \xi_0^2 \left(\partial_x - \frac{i}{2q_c} \partial_y^2 \right)^2, \quad \text{for } \mathbf{q}_c = (q_c, 0), \quad (7a)$$

$$\mathcal{L} = \mathcal{L}_{\perp}^2 := \xi_0^2 \left(\partial_y - \frac{i}{2q_c} \partial_x^2 \right)^2, \quad \text{for } \mathbf{q}_c = (0, q_c). \quad (7b)$$

The coherence length ξ_0 and the nonlinear coefficient g for the Brusselator in the special case of $D = a^2$ are $\xi_0^2 = 1$ and $g = 3/(2a^2)$ [35].

Control parameter drop. We introduce the control parameter drop by assuming the spatially dependent control parameter $\beta(x, \delta_x)$:

$$\beta = \beta_0 + \frac{M}{2} \left[\tanh \left(\frac{x - x_l}{\delta_x} \right) - \tanh \left(\frac{x - x_r}{\delta_x} \right) \right]. \quad (8)$$

We assume $L := x_r - x_l \gg \lambda_c$ and $\beta_0 < 0$. M and β_0 are chosen such that the maximum value $\beta_m = \beta_0 + M$ is small and positive. Then $\beta(x, \delta_x)$ is supercritical in the subdomain $\bar{x}_l < x < \bar{x}_r$, where

$$\bar{x}_{l,r} = x_{l,r} \pm \frac{\delta_x}{2} \ln \left(\frac{-\beta_0}{M + \beta_0} \right), \quad (9)$$

and drops down to the subcritical value β_0 outside this domain. The steepness of the control parameter drop around $\bar{x}_{l,r}$ increases with decreasing values of the drop width δ_x .

For small values of δ_x , the control parameter $\beta(x, \delta_x)$ varies rapidly in a narrow range around $\bar{x}_{l,r}$. However, only the slowly (adiabatically) varying contributions to $\beta(x, \delta_x)$ affect the solutions of amplitude equations. The rapidly (non-adiabatically) varying part is smoothed out and must be treated separately. We therefore decompose

$\beta(x, \delta_x)$ into an adiabatic and non-adiabatic part. For this purpose, we introduce the slow length scale $\delta_A := 2\xi_0/\sqrt{\beta_m} > \delta_x$ and choose $\beta_0 = -\varepsilon$, $M = 2\varepsilon$ (where ε is positive and small). We then express the slowly varying contribution $B_0(x)$ via eq. (8) by choosing $\delta_x = \delta_A$:

$$B_0(x) = \beta(x, \delta_A). \quad (10)$$

The difference between $\beta(x, \delta_x)$ and $B_0(x)$ becomes small in the centre of $[x_l, x_r]$ and takes its largest values around $x_{l,r}$. We expand the rapidly varying difference $\beta(x, \delta_x) - B_0(x)$ into a series to obtain

$$\begin{aligned} \beta(x, \delta_x) = B_0(x) + \frac{M}{2} \sum_m \left\{ B_m^l(x) \sin[mq_c(x - x_l)] \right. \\ \left. + B_m^r(x) \sin[mq_c(x - x_r)] \right\}, \end{aligned} \quad (11)$$

where $m = n/N_L$, $n \in N$ and $N_L = L/\lambda_c$. The functions $B_m^{l,r}(x)$ are localised around $x_{l,r}$ and we choose a Gaussian for their representation:

$$B_m^{l,r}(x) = \hat{B}_m^{l,r} \exp\left[-\frac{(x - x_{l,r})^2}{\delta_{G,m}^2}\right]. \quad (12)$$

The Gaussian amplitudes $\hat{B}_m^{l,r}$ and their widths $\delta_{G,m}$ are determined via a correlation analysis. We calculate the correlation function between the rapidly varying part

$$\Delta\tilde{\beta}(x, \delta) = \tanh(x/\delta) - \tanh(x/\delta_A) \quad (13)$$

and the test function

$$f_m(x, \delta_{\text{test}}) = \frac{1}{\sqrt{\pi}\delta_{\text{test}}} e^{-x^2/\delta_{\text{test}}^2} \sin(mq_c x). \quad (14)$$

We then choose the Gaussian width $\delta_{G,m}$ to be the value of δ_{test} that maximises the correlation function. The amplitudes $\hat{B}_m^{l,r}$ are calculated via the overlap integral between $f_m(x, \delta_{G,m})$ and $\Delta\tilde{\beta}$. Figure 2(a) shows the contributions $B_m^l := \varepsilon B_m^l(x) \sin(mq_c x)$ for $m = 1, 2$ in comparison to the full shape of $\beta(x, \delta_x)$. Both functions are localised around $x_l = 0$ and approach zero within a short range ($\ll \delta_A$) around the control parameter drop. The Gaussian amplitudes $\hat{B}_1^{l,r}$ and $\hat{B}_2^{l,r}$ decrease as a function of the drop width δ_x (fig. 2(b)). These non-adiabatic contributions vanish for $\delta_x > \delta_A$. The amplitude $\hat{B}_1^{l,r}$ is usually larger than $\hat{B}_2^{l,r}$, except in the limit of very small drop widths.

The patterns in fig. 1 are obtained for a rectangular supercritical subdomain of the control parameter in the form

$$\begin{aligned} \beta = \beta_0 + \frac{M}{4} \left[\tanh\left(\frac{x - x_l}{\delta_x}\right) - \tanh\left(\frac{x - x_r}{\delta_x}\right) \right] \\ \times \left[\tanh\left(\frac{y - y_b}{\delta_y}\right) - \tanh\left(\frac{y - y_t}{\delta_y}\right) \right]. \end{aligned} \quad (15)$$

Here, we introduced a second drop width δ_y to describe the additional spatial dependence of β in the y -direction. $\beta(x, y, \delta_x, \delta_y)$ is supercritical in the two-dimensional area $[\bar{x}_l, \bar{x}_r] \times [\bar{y}_b, \bar{y}_t]$.

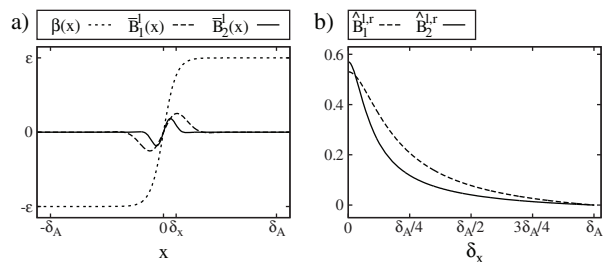


Fig. 2: (a) Contributions $\bar{B}_1^l(x)$ and $\bar{B}_2^l(x)$ to the control parameter drop $\beta(x, \delta_x)$ for $\delta_x = 0.11\delta_A$. (b) Gaussian amplitudes $\hat{B}_1^{l,r}$ and $\hat{B}_2^{l,r}$ of the localised amplitudes as a function of the drop width δ_x for $\varepsilon = 0.05$.

Non-adiabatic effects cause an orientational transition. – We now include the control parameter drop into the amplitude equation using the decomposition given in eq. (11). The control parameter β in eq. (6) is replaced by the slowly (adiabatically) varying part $B_0(x)$ as given by eq. (10). The short-wavelength contributions $\propto B_m^{l,r}(x) \exp(imq_c x)$ with $m = 1, 2, 3, 4$ in eq. (11) cause additional (non-adiabatic) terms in the amplitude equation for parallel stripes [37]. It then takes the form

$$\begin{aligned} \partial_t A = B_0(x)A + \mathcal{L}_{\parallel}^2 A - g|A|^2 A \\ + \sum_{m=1}^4 \alpha_m B_m(x) (A^*)^{m-1}. \end{aligned} \quad (16)$$

Here, α_m are constant parameters depending on the respective system. The complex localised contributions $B_m(x)$ due to the control parameter drop are given by

$$B_m(x) = i \frac{M}{4} [B_m^l(x) e^{-imq_c x_l} - B_m^r(x) e^{-imq_c x_r}]. \quad (17)$$

The magnitudes of $B_1(x)$ and $B_2(x)$ are similar, as shown in fig. 2. The coefficient $B_2(x)$ reduces the threshold of the pattern onset [37]. $B_1(x)$ changes the supercritical bifurcation (in the case $B_1 = 0$) into an imperfect one [37,38] and, therefore, has a stronger impact than $B_2(x)$. The effects caused by $B_{3,4}(x)$ are restricted to the post-threshold regime and are much smaller than $B_{1,2}(x)$. Hence, they are neglected henceforth. Equation (16) can be derived from the functional

$$\begin{aligned} F_{\parallel} = \int dx dy \left[-B_0(x)|A|^2 + \frac{g}{2}|A|^4 + |\mathcal{L}_{\parallel} A|^2 \right. \\ \left. - \sum_{m=1}^2 \frac{\alpha_m}{m} (B_m(x)A^{*m} + B_m^*(x)A^m) \right] \end{aligned} \quad (18)$$

via $\partial_t A = -\delta F_{\parallel}/\delta A^*$. For the Brusselator in the case $D = a^2$, we find $\alpha_1 = 2a$ and $\alpha_2 = 5/3$.

The amplitude equation for perpendicular stripes with $\mathbf{q}_c = (0, q_c)$ is not affected by resonance contributions $\propto B_m$. It is described by eq. (6) with $\mathcal{L} = \mathcal{L}_{\perp}^2$ as given in eq. (7b) and the slowly varying control parameter

$\beta = B_0(x)$, cf. eq. (10). The related functional is

$$F_{\perp} = \int dx dy \left[-B_0(x)|A|^2 + \frac{g}{2}|A|^4 + |\mathcal{L}_{\perp}A|^2 \right]. \quad (19)$$

For small values of δ_x , the coefficients $B_{1,2}$ have considerable magnitude (fig. 2(b)). However, the related non-adiabatic effects only affect the amplitude equation for parallel stripes, cf. eq. (16). Due to the imperfect bifurcation, parallel stripes already have a finite amplitude below the bulk threshold $\beta_m = 0$, especially around $x_{l,r}$, where $B_{1,2}$ take the largest values. This finite amplitude A decreases the functional F_{\parallel} for parallel stripes with respect to F_{\perp} . Thus, for small values of δ_x , parallel stripes are preferred compared to perpendicular stripes.

For large values of δ_x , the non-adiabatic contributions $B_{1,2}$ become small and can be neglected (fig. 2(b)). In this case, the amplitude equations and the functionals for the two different stripe orientations only differ in the linear operator. These include different orders of derivatives in the x -direction: $|\partial_x A|^2$ in the functional for parallel stripes, eq. (18), and $|\partial_x^2 A|^2$ for perpendicular stripes, eq. (19). Thus, spatial variations of the amplitude $A(\mathbf{r}, t)$ affect the two functionals differently. The slow spatial variation of the control parameter $B_0(x)$ in the x -direction is reflected in a spatial variation of the amplitude $A(\mathbf{r}, t)$. This increases both functionals. However, due to the different orders of x -derivatives, the functional for perpendicular stripes has a lower value [3,39]. Therefore, perpendicular stripes will be preferred for large δ_x .

According to this reasoning, we predict stripes aligned perpendicular to the supercritical border for a large drop width δ_x and parallel for small δ_x . Therefore, we expect an orientational transition for medium values of δ_x . Note, for these considerations only the contributions B_0 , B_1 and B_2 to the decomposition in eq. (11) are taken into account. However, the predicted orientational transition of stripes is rather insensitive to these approximations as confirmed by simulations of the Brusselator in the next section.

Numerical results for the Brusselator. – In the previous part we found an orientational transition of stripe patterns by changing the width of control parameter drops. This prediction is based on a reasoning including approximations. Therefore, the effect is verified by simulations of the Brusselator model, cf. eqs. (1), with supercritical subdomains of width $L = 20\lambda_c$, embedded in larger subcritical domains with overall system sizes $l_{x,y}$. The model is solved using a common pseudospectral method with periodic boundary conditions [40] and $N_{x,y}$ modes, respectively. We choose $\beta_0 = -0.05$ and perturb the basic solution by small amplitude random noise.

For large widths δ_x of control parameter drops, *i.e.* slow variations of the control parameter, the preferred orientation of a stripe pattern is nearly perpendicular to the borders of the supercritical domain, *i.e.* $\mathbf{q} \sim (0, q_c)$, as shown in fig. 3 for $\delta_x = 5\lambda_c$. This confirms the prediction in terms of the amplitude equations in the previous section



Fig. 3: Stripes favour a perpendicular orientation with respect to shallow control parameter drops ($\delta_x = 5\lambda_c$). Simulation of the Brusselator started at $\beta_m = 0.001$ and was slowly increased to $\beta_m = 0.05$. Parameters: $l_x = l_y = 50\lambda_c$, $N_x = N_y = 1024$. Note: only a cutout of the simulation is shown.

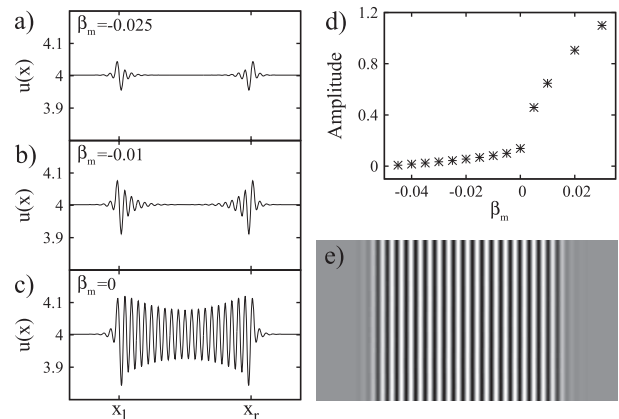


Fig. 4: Simulations of the Brusselator model with a narrow control parameter drop ($\delta_x = 0.5\lambda_c$). Cross-sections of the two-dimensional stripe pattern for (a) $\beta_m = -0.025$, (b) $\beta_m = -0.01$, (c) $\beta_m = 0$. (d) The stripe amplitude as a function of β_m implies an imperfect bifurcation. (e) Snapshot of the parallel stripes for $\beta_m = 0.02$. Simulation parameters: $l_x = 50\lambda_c$, $l_y = 25\lambda_c$, $N_x = 1024$, $N_y = 512$.

(for similar results for periodic modulations in extended systems see ref. [41]). Similar orientations are obtained for drop widths down to about $\delta_x \simeq \lambda_c$.

For small δ_x , *e.g.* $\delta_x = 0.5\lambda_c$, the stripes align parallelly to the borders of the supercritical range, *i.e.* $\mathbf{q}_c \sim (q_c, 0)$, as in fig. 4(e) for $\beta_m = 0.02$. Moreover, localised Turing stripe patterns of finite amplitude occur around the borders at $x_{l,r}$ already at subcritical values of β_m (see cross-sections in fig. 4(a) and (b)). For increasing β_m , they expand into the whole supercritical domain. At the bulk threshold $\beta_m = 0$ (fig. 4(c)) the stripes already have a finite amplitude throughout the range $[x_l, x_r]$. The maximum stripe amplitude of the stationary solution as a function of β_m is shown in the bifurcation diagram in fig. 4(d). The form of the bifurcation is imperfect, as expected from the analysis on the basis of the amplitude equations in the previous section.

The two different preferred stripe orientations for large $\delta_x = 5\lambda_c$ in fig. 3 and small $\delta_x = 0.5\lambda_c$ in fig. 4 clearly confirm an orientational transition of stripes in the

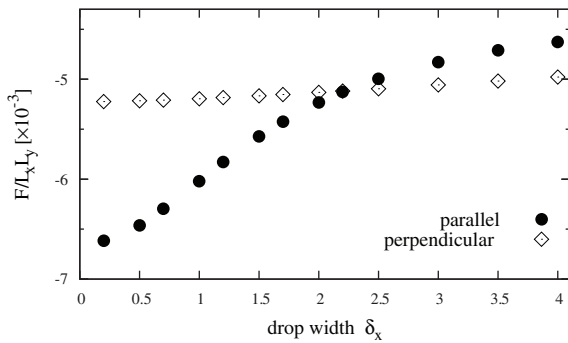


Fig. 5: Comparison of the functional for stripes as a function of the drop width δ_x with the stripe wave vector $\mathbf{q}_c = (0, q_c)$ (filled circles) and $\mathbf{q}_c = (q_c, 0)$ (open diamonds). Parameters: $\beta_0 = -0.05$, $M = 0.1$.

supercritical domain depending on the width of the control parameter drop along its border.

We can further restrict the domain size by varying the control parameter simultaneously along the x - and y -direction, cf. eq. (15). In these rectangular domains¹, one can combine different drop widths δ_x and δ_y to trigger different stripe orientations as shown by four examples in fig. 1. Combining, *e.g.*, large drop widths at the long side of the rectangle with small drop widths at the short side creates a remarkably uniform stripe pattern, cf. fig. 1(d). Using different combinations of $\delta_{x,y}$ may be a promising tool for designing Turing patterns in localised light-sensitive chemical reactions [42].

Orientational transition regime. – The orientational transition of stripes is deduced in terms of amplitude equations and confirmed by numerical simulations of the Brusselator model. The amplitude equations can be derived from the functionals, eqs. (18) and (19). Calculating these functionals as a function of the drop width allows to determine the preferred orientation for this δ_x . In the range where $F_\perp < F_\parallel$, a perpendicular stripe orientation is expected and vice versa. For this purpose, we perform simulations of the amplitude equations for the two stripe orientations using the aforementioned pseudospectral algorithm (simulation parameters: $l_x = l_y = 50\lambda_c$, $N_x = N_y = 1024$, $L = 20\lambda_c$, $\beta_0 = -0.05$, $\beta_m = 0.05$). When the solutions reach the stationary state, the functionals displayed in fig. 5 are calculated.

The functional corresponding to perpendicular stripes in eq. (19) does not contain the non-adiabatic contributions B_1 and B_2 to the control parameter drop. Regardless of the assumptions made for the justification of eq. (19) and the related amplitude equation, one may use $\beta(x, \delta_x)$ instead of $B_0(x)$. The functional then deviates only slightly from its constant value in the case of $B_0(x)$. In addition, fig. 5 shows that the functional with $\beta(x, \delta_x)$ is nearly independent of δ_x , *i.e.* stripes perpendicular to

¹Simulation parameters: $\beta_0 = -0.1$, $\beta_m = 0.05$, $L_x = 30\lambda_c$, $L_y = 20\lambda_c$, $l_x = 60\lambda_c$, $l_y = 50\lambda_c$, $N_x = N_y = 1024$.

the border of the supercritical range are rather insensitive to the width δ_x .

For parallel stripes, $\mathbf{q} = (q_c, 0)$, the resonance effects covered by B_1 (and B_2) are relevant and the associated functional is given in eq. (18). The two functionals for the two different stripe orientations are shown as a function of the drop width δ_x in fig. 5. For narrow control parameter drops, *i.e.* δ_x small, the functional for parallel stripes is significantly lower. Thus, the parallel orientation is preferred. However, the functional for parallel stripes strongly increases as a function of the drop width. The orientational transition takes place at the intersection of the two functionals. For larger δ_x , the perpendicular orientation of the stripes is preferred.

Summary and conclusions. – In this work, we identified and investigated a new class of finite pattern forming systems confined by control parameter drops from super- to subcritical values. These orient stripe patterns even without boundary conditions for the relevant fields. The stripe orientation depends on the width of the control parameter drops. We found a novel *orientational transition of stripe patterns* with respect to the borders as a function of the width of control parameter drops.

In light-sensitive chemical reaction-diffusion systems showing Turing patterns [30,31] the transition length between the patterns (supercritical) and the homogeneous state (subcritical) may be varied by the length of a smooth transition between illuminated and dark areas.

The Swift-Hohenberg (SH) model [43] is, besides the Brusselator a further paradigmatic model for studying the formation of spatially periodic patterns [2,3]. It behaves differently with respect to control parameter drops along the border of a supercritical domain. The basic state of the Brusselator is a function of the control parameter b , cf. eq. (2). Therefore, control parameter drops change the basic state of the bifurcation to Turing patterns. In the case of steep control parameter drops, the bifurcation to parallel stripes becomes imperfect, causing a different orientation than for smooth control parameter variations. In contrast, the basic state $u_h = 0$ of the SH model remains unchanged for spatially varying control parameters. The onset of periodic patterns is reduced but the bifurcation remains perfect. The local 1:2 resonance occurring in the case of a steep control parameter drop is not sufficient to change the stripe orientation like for the Brusselator. The same applies to the mean-field model for block copolymers (see, *i.e.*, [44]). Therefore, we do not find the aforementioned orientational transition of stripe patterns in the SH or the block copolymer model. However, in common systems where the basic state is also changed by control parameter variations, orientational transitions of stripe patterns are very likely.

Our results for stationary patterns may also be important for traveling waves that occur, for instance, in the cell biological MinE/MinD protein reaction on flat substrates [12,29]. To mimic the effects of cell confinement

in such extended experiments, reactive membranes were created in subdomains of the substrate [29,45]. In this way, the traveling waves are restricted to the range above the functionalised parts of the membrane. These may be interpreted as subdomains with a supercritical control parameter. In this experiment the traveling waves align perpendicularly to the borders of the functionalised area [29]. It is very likely that this orientational behaviour is again governed by generic principles similar to those discussed in this work and specific molecular reaction schemes or three-dimensional effects provide quantitative modifications [29,46,47]. Is the complex behavior of MinE/MinD oscillations in further restricted domains, as investigated recently in ref. [48], determined by the specific properties of the kinetic reaction models? Or do again generic principles of pattern formation play a leading role as described in this work?

Enlightening discussions with M. HILT and M. WEIß are gratefully acknowledged.

REFERENCES

- [1] BALL P., *The Self-Made Tapestry: Pattern Formation in Nature* (Oxford University Press, Oxford) 1998.
- [2] CROSS M. C. and GREENSIDE H., *Pattern Formation and Dynamics in Nonequilibrium Systems* (Cambridge University Press, Cambridge) 2009.
- [3] CROSS M. C. and HOHENBERG P. C., *Rev. Mod. Phys.*, **65** (1993) 851.
- [4] LAPPA M., *Thermal Convection: Patterns, Evolution and Stability* (Wiley, New York) 2010.
- [5] WEISS S., SEIDEN G. and BODENSCHATZ E., *New J. Phys.*, **14** (2012) 053010.
- [6] BODENSCHATZ E., ZIMMERMANN W. and KRAMER L., *J. Phys. (Paris)*, **49** (1988) 1875.
- [7] KRAMER L. and PESCH W., *Annu. Rev. Fluid Mech.*, **27** (1995) 515.
- [8] KAPRAL R. and SHOWALTER K. (Editors), *Chemical Waves and Patterns* (Springer, The Netherlands) 1995.
- [9] MIKHAILOV A. S. and SHOWALTER K., *Phys. Rep.*, **425** (2006) 79.
- [10] BEN-JACOB E., SHOCHET O., TENENBAUM A., COHEN I., CZIROK A. and VICSEK T., *Nature*, **368** (1994) 46.
- [11] KONDO S. and MIURA T., *Science*, **329** (2010) 1616.
- [12] LOOSE M., FISCHER-FRIEDRICH E., RIES J., KRUSE K. and SCHWILLE P., *Science*, **320** (2008) 789.
- [13] MERON E., *Nonlinear Physics of Ecosystems* (CRC Press, Boca Raton) 2015.
- [14] KRAMER L. and HOHENBERG P. C., *Physica D*, **13** (1984) 357.
- [15] GREENSIDE H. and COUGHRAN W. M., *Phys. Rev. A*, **30** (1984) 398.
- [16] KRAMER L., HOHENBERG P. C. and RIECKE H., *Physica D*, **15** (1985) 402.
- [17] CROSS M. C., *Phys. Fluids*, **25** (1982) 936.
- [18] BAJAJ K. M., MUKOLOBWIEZ N., CURRIER N. and AHLERS G., *Phys. Rev. Lett.*, **83** (1999) 5282.
- [19] CHIAM K.-H., PAUL M. R., CROSS M. C. and GREENSIDE H., *Phys. Rev. E*, **67** (2003) 056206.
- [20] CROSS M. C., DANIELS P. G., HOHENBERG P. C. and SIGGIA E. D., *J. Fluid Mech.*, **127** (1983) 155.
- [21] CROSS M. C., *Phys. Rev. Lett.*, **57** (1986) 2935.
- [22] CROSS M. C., *Phys. Rev. A*, **38** (1988) 3593.
- [23] MOSES E., FINEBERG J. and STEINBERG V., *Phys. Rev. A*, **35** (1987) 2757.
- [24] KOLODNER P. and SURKO C. M., *Phys. Rev. Lett.*, **61** (1988) 842; KOLODNER P., *Phys. Rev. A*, **44** (1991) 6448.
- [25] GARNIER N., CHIFFAUDEL A. and DAVIAUD F., *Physica D*, **174** (2003) 30.
- [26] KRAMER L., BEN-JACOB E., BRAND H. and CROSS M. C., *Phys. Rev. Lett.*, **49** (1982) 1891.
- [27] CROSS M. C., *Phys. Rev. A*, **29** (1984) 391.
- [28] RIECKE H., *Europhys. Lett.*, **2** (1986) 1.
- [29] SCHWEIZER J., LOOSE M., BONNY M., KRUSE K., MÖNCH I. and SCHWILLE P., *Proc. Natl. Acad. Sci. U.S.A.*, **109** (2012) 15283.
- [30] MUNUZURI A. P., DOLNIK M., ZHABOTINSKY A. M. and EPSTEIN I. R., *J. Am. Chem. Soc.*, **121** (1999) 8065.
- [31] DOLNIK M., BERENSTEIN I., ZHABOTINSKY A. M. and EPSTEIN I. R., *Phys. Rev. Lett.*, **87** (2001) 238301.
- [32] PRIGOGINE I. and LEFEVER R., *J. Chem. Phys.*, **48** (1968) 1695.
- [33] NICOLIS G. and PRIGOGINE I., *Self-Organization in Nonequilibrium Systems, from Dissipative Structures to Order through Fluctuations* (Wiley, New York) 1977.
- [34] WALGRAEF D., *Spatio-Temporal Pattern Formation* (Springer, New York) 1997.
- [35] PENA B. and PEREZ-GARCIA C., *Phys. Rev. E*, **64** (2001) 056213.
- [36] NEWELL A. C. and WHITEHEAD J. A., *J. Fluid Mech.*, **38** (1969) 279.
- [37] COULLET P., *Phys. Rev. Lett.*, **56** (1986) 724.
- [38] PETER R. *et al.*, *Phys. Rev. E*, **71** (2005) 046212.
- [39] MALOMED B. A. and NEPOMNYASHCHY A. A., *Europhys. Lett.*, **21** (1993) 195.
- [40] KOPRIVA D. A., *Implementing Spectral Methods for Partial Differential Equations* (Springer, The Netherlands) 2009.
- [41] FREUND G., PESCH W. and ZIMMERMANN W., *J. Fluid Mech.*, **673** (2011) 318.
- [42] STEINBOCK O., KETTUNEN P. and SHOWALTER K., *Science*, **269** (1995) 1857.
- [43] SWIFT J. B. and HOHENBERG P. C., *Phys. Rev. A*, **15** (1977) 319.
- [44] WEITH V., KREKHOV A. and ZIMMERMANN W., *J. Chem. Phys.*, **139** (2013) 054908.
- [45] LAGNY T. J. and BASSEREAU P., *Interface Focus*, **5** (2015) 20150038.
- [46] HALATEK J. and FREY E., *Cell Rep.*, **1** (2012) 741.
- [47] HALATEK J. and FREY E., *Proc. Natl. Acad. Sci. U.S.A.*, **111** (2014) E1817.
- [48] WU F., VAN SCHIE B. G. C., KEYNER J. E. and DEKKER C., *Nat. Nanotechnol.*, **10** (2015) 719.